

HARD X-RAY IMAGING OF THE GALACTIC BLACK HOLE CANDIDATE GX 339–4

C. E. COVAULT,¹ J. E. GRINDLAY, AND R. P. MANANDHAR
 Center for Astrophysics, 60 Garden Street, Mail Stop 6, Cambridge MA 02138
 Received 1991 October 31; accepted 1992 January 9

ABSTRACT

Imaging and spectral observations in the energy range 20–250 keV of the black hole candidate GX 339–4 have been obtained with the Energetic X-ray Imaging Telescope Experiment (EXITE). Observations were made during a balloon flight from Alice Springs, Australia on UT 1989 May 8–10. A single source of nearly 6σ significance is detected near the center of the $3^{\circ}4'$ field of view with a position consistent with GX 339–4. This is the first imaging observation of GX 339–4 at hard X-ray energies. Our result confirms previously reported results from nonimaging experiments showing significant hard X-ray flux up to $\gtrsim 60$ keV, with a power-law spectral fit similar to other black hole candidates such as Cygnus X-1. The source may have been in an outburst state similar to that recently detected with BATSE on *GRO*.

Subject headings: binaries: general — black hole physics — stars: variables: other — telescopes — X-rays: stars

1. INTRODUCTION

Only three X-ray binaries have been identified as convincing black hole candidates based upon dynamical evidence for a mass of the compact object of greater than $3 M_{\odot}$ (e.g., McClintock 1991). Since such dynamical identification of black hole (BH) binaries remains difficult, we are motivated to examine the properties of the emitted X-rays themselves in search of characteristic signatures that might generally distinguish black hole binaries from accreting neutron stars. One such possible signature, based primarily on the X-ray properties of the archetypical black hole candidate Cygnus-1, is the presence of a strong flux of hard X-rays in the form of a power-law tail extending to ~ 100 keV or more. (See, for example, Liang & Nolan 1984.) In this picture, hard X-rays are produced within some optically thin Comptonizing region of hot electrons near the inner edge of the accretion disk. Such a hot inverse Compton region might be expected to form near an accreting black hole as opposed to a neutron star where the strong ~ 1 keV thermal X-rays from the stellar surface would rapidly quench, by Compton cooling, any hot corona. In order to test this association further, and to remove any ambiguity of source identification in crowded Galactic bulge fields, we have carried out coded-aperture imaging and spectra (20–250 keV) of the BH candidate GX 339–4.

2. OBSERVATIONS

We have observed GX 339–4 with our Energetic X-ray Imaging Telescope Experiment (EXITE) during a ~ 30 hr balloon flight 1989 May 8–10 from Alice Springs, Australia. GX 339–4 was observed from UT 1555 to 1730 on May 9. Preliminary detection results from these observations were reported previously (Covault, Grindlay, & Manandhar 1990a; Covault, Manandhar, & Grindlay 1991b). Here we present a more complete analysis which confirms our preliminary reports.

The EXITE balloon-borne X-ray telescope is designed for high-resolution imaging in the 20–300 keV energy band, using the coded-aperture imaging technique. The design and per-

formance of the instrument have been summarized previously (Grindlay et al. 1986; Garcia et al. 1986; Braga, Covault, & Grindlay 1989; Covault et al. 1990a, b, 1991a). Briefly, the EXITE position-sensitive X-ray detector consists of a 34.5 cm diameter, 6.4 mm thick NaI(Tl) scintillation crystal bonded to the curved entrance window of a large, two-stage image intensifier tube. The second stage has a two-dimensional silicon PIN diode readout. The detector system is contained within a graded cylindrical passive shield surrounded on all sides by an active shield of plastic scintillator to reject charged particle and Compton-scattered background. Imaging is accomplished by a rectangular Uniformly Redundant Array (URA) (Fenimore & Cannon 1978) coded-aperture mask located 2 m in front of the detector. The URA mask is an extended 11×13 pattern with a 13 mm square element size, yielding $22'$ imaging resolution within a $3^{\circ}4'$ field of view defined by crossed one-dimensional collimators. The telescope alt-az pointing system on the gondola is stabilized to $\sim 1'$ by a two high-speed gyros (azimuth and elevation) for inertial reference. Absolute telescope elevation is read out by a shaft encoder and inclinometer with $6'$ resolution. Absolute azimuth pointing is accomplished with two magnetometers in coordination with ground calculations to compensate for local magnetic field fluctuations. Fine target acquisitions (az and el), inertial drift corrections (during flight), and postflight aspect reconstruction are made with two co-aligned on-board TV cameras (nighttime) and a Sun-tracking system (daytime) (Grindlay et al. 1990).

GX 339–4 images were constructed (cf. Covault 1991) from data collected within the central 14 cm radius of the detector, where the accuracy of flat-fielding and of the electronics gain and offset calibrations have been demonstrated from observations of the Crab (Covault 1991). Pointing aspect information from the co-aligned intensified TV was applied to each individual observation segment of ~ 4 minutes. The resulting images were summed after applying an appropriate pointing correction accurate to within $\sim 6'$ relative to the start of the observation. There is a $\sim 16'$ overall smearing in the summed images due to the field rotation, of about 45° , during the 1.5 hr observation.

Stacked images were constructed in several energy bands and searched for significant peaks. The strongest candidate

¹ Now at The Enrico Fermi Institute, The University of Chicago, 5640 South Ellis Avenue, Chicago IL 60637.

TABLE 1
DETECTED FLUX FROM EACH ENERGY BAND IN IMAGE OF GX 339-4

Energy Band	Energy Range (keV)	Raw Imaged Counts	Flux * E ² (photons s ⁻¹ cm ⁻² keV ⁻¹) * (keV) ²	Flux (mCrab*)
0.....	20-29	155 ± 117	1.12 ± 0.84	170
1.....	29-36	142 ± 66	0.85 ± 0.40	140
2.....	36-48	324 ± 91	1.28 ± 0.36	220
3.....	48-63	548 ± 106	1.63 ± 0.32	280
4.....	63-82	78 ± 202	0.20 ± 0.32	30
5.....	82-111	297 ± 235	0.60 ± 0.48	110
6.....	111-153	526 ± 337	1.18 ± 0.75	220
7.....	153-255	520 ± 578	1.41 ± 1.20	280

NOTE.—Photon fluxes are multiplied by the mean energy squared for each energy band.

* Flux is given in units relative to the flux of the Crab X-ray source (1 Crab = 1000 mCrab = $8.6E^{-2.1}$ photons s⁻¹ cm⁻² keV⁻¹).

source peak (5.9σ) is shown in Figure 1, which is the reconstructed image of the source as seen in bands 1 and 2 combined (36–63 keV). Other bands also show a statistically weak positive flux relative to background at this location on the image but do not improve the significance of the candidate peak. Table 1 lists the raw imaged counts detected in each energy band and the net photon flux determined from our model of the effective area and energy response of the detector.

The indicated cross on the image (Fig. 1) represents the constraints on the absolute location of GX 339-4 in the field of view based upon the uncertainties in the boresighting of the telescope with the elevation and azimuth aspect systems. The azimuth “error bar” represents the relatively large alignment uncertainty between the TV and telescope axes because no

other bright sources were observable during the nighttime portion of the flight to boresight the TV/telescope alignment. The elevation “error bar” represents uncertainty in the elevation shaft angle relative to the local vertical.

While the absolute azimuth aspect uncertainty is fairly large, the elevation constraint alone is enough to give us reasonable confidence that we are detecting the source GX 339-4. We have used the analysis of Finger (1987) (which we have confirmed through extensive simulations) to estimate the probability of detecting a peak above 5.5σ significance within a given region of the image plane. This analysis searches for peaks within each resolution region of the image ($\sim 20' \times 20'$) and calculates the a priori probability of detecting peaks within each region, assuming that the peak resulted from a noise fluctuation during an observation of a uniform background field. The probability (adjusted for trials in combining energy bands) of detecting such a peak within $20'$ of the expected GX 339-4 elevation is only 0.04%.

Although our image formally locates the source to be within a preliminary “boresight box” of $\sim 20' \times 60'$, if we use the offsets derived from Figure 1 to compute a final boresight, we detect a source in our observation of the Galactic center (cf. Covault et al. 1991b for a preliminary report) within a $\sim 10'$ radius of the expected position of 1E 1740.7-2942 (Skinner et al. 1991). As $10'$ is within the source localization errors due to centroiding ($\sim 7'$) and relative aspect ($\sim 6'$), the two source positions are consistent, giving us further confidence that we have identified GX 339-4 correctly and that no other source is responsible for hard X-ray emission within the imaged region.

We derive the best-fit spectral index by fitting the detected counts to the number predicted from folding power-law incident flux models through the complete telescope and detector response (Covault 1991). Figure 2 shows the best fit for a power-law spectrum of the form $F = C(E/55 \text{ keV})^{-\alpha}$ photons cm⁻² s⁻¹ keV⁻¹. The inset in Figure 2 shows the χ^2 contour map for the two-parameter fit, which yields a spectral index $\alpha = 2.2 \pm 0.7$ and a flux normalization, $C = 2.9 \pm 0.6 \times 10^{-4}$.

3. DISCUSSION

The BH candidate GX 339-4 was observed above 20 keV by the *Ariel 6* and *OSO 8* satellites (Ricketts 1982; Dolan et al. 1987) and several times by *HEAO 1 A-4* (Nolan et al. 1982). The hard X-ray flux has been shown to vary by factors of ~ 3 –10 and has typically been well described by a power law above 20 keV with a best-fit photon index ranging from 0.9 to 2.3, but generally consistent with 2.0. All of these nonimaging detectors have had fields of view $\gtrsim 1^\circ$ – 2° . The imaging information provided by EXITE confirms that the previous nonimaging hard X-ray results are associated with GX 339-4 only and have not been contaminated by some unknown nearby source of comparable strength outside a $\sim 20'$ radius.

Such a localization is important for hard X-ray sources, particularly for sources located in the crowded Galactic bulge. GX 5-1, for example, was misassociated with a nearby hard X-ray imaging SIGMA telescope aboard the *GRANAT* spacecraft (Sunyaev et al. 1991a). The EXITE detection of GX 339-4 represents the first imaging detection of GX 339-4 at hard X-ray energies.

Figure 2 shows the spectrum observed by EXITE compared to spectral fits obtained during selected observations from observations with *Ariel 6*, *OSO 8*, and *HEAO 1*. (Spectral varia-

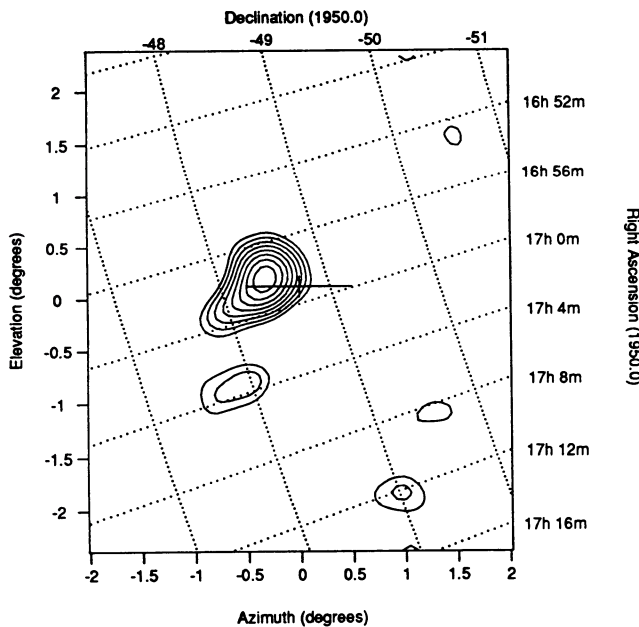


FIG. 1.—The EXITE image of the Galactic black hole candidate, GX 339-4 from 36 to 63 keV, detected with a significance of 5.9σ . The contour intervals represent significance steps from 2 to 6σ in 0.5σ steps. The 2.5σ bumps and northern extension of the main peak are probably noise fluctuations. The cross indicates constraints on the absolute position of GX 339-4 based upon TV and elevation boresight determination and is centered (for start of observation) at the optical position (Grindlay et al. 1978) for GX 339-4, which is $\alpha_{1950} = 16^{\text{h}}59^{\text{m}}01^{\text{s}}.9$, $\delta_{1950} = -48^{\circ}43'06''$.

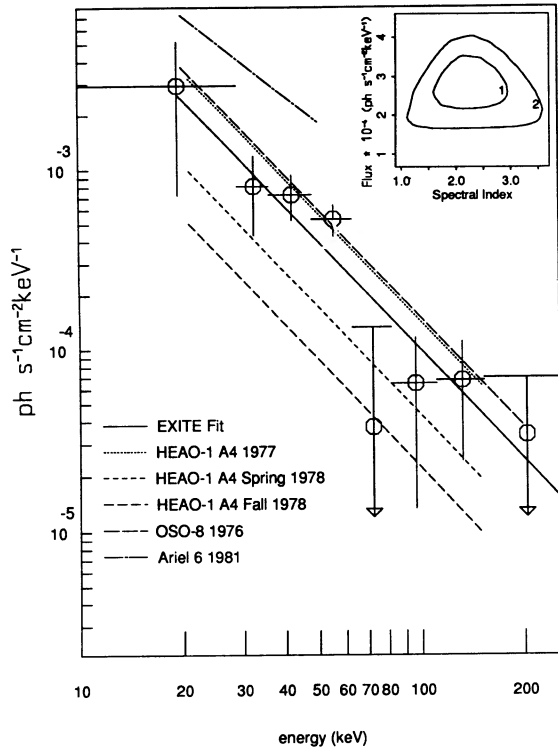


FIG. 2.—EXITE spectrum (points and solid line) for GX 339-4 vs. sample spectra (dotted lines) as measured by a previous nonimaging experiments, *HEAO 1 A-4* (Nolan et al. 1982), *Ariel 6* (Ricketts 1982), and *OSO 8* (Dolan et al. 1987). The inset shows χ^2 contours (1 σ , 2 σ) for the best-fit EXITE spectral index and flux normalization.

bility is observed in all three satellite observations.) Our results are consistent with the reported flux range of hard X-rays and a power-law tail, and therefore support the black hole candidacy of this source. EXITE flux measurements, which yield

$L_{20-100 \text{ keV}} \sim 6 \times 10^{36} \text{ ergs s}^{-1}$ assuming a distance of 4 kpc, are fairly well matched to the *HEAO A-4* spectrum observed (Nolan et al. 1982) while the source was in a “high” state for hard X-rays. Nearly contemporaneous *Ginga* All-Sky Monitor data indicate that GX 339-4 was in a high state in soft X-rays (with a nearly constant 6–20 keV component) during 2 months of visibility up through 1989 April 15 (Miyamoto et al. 1991). Very recently, a significant increase in flux from GX 339-4 has been observed during the period 1991 July–September by the BATSE instrument aboard the *Gamma Ray Observatory* (Fishman et al. 1991a, b) and the SIGMA telescope aboard the *GRANAT* spacecraft (Sunyaev et al. 1991b). These observations indicate a dramatic increase (up to 300–400 mCrab) in the 40–150 keV energy region and a spectral index of 2.1–2.4. Our observations, at about 180 mCrab in the same band and the same spectral index, may indicate a similar outburst was in progress. The 1978 fall *HEAO A-4* and 1981 *Ariel 6* spectra (Fig. 2) indicate that such hard X-ray outbursts may be common.

To distinguish between outburst and quiescence models we need tighter constraints and localization of any break in the power-law spectrum. We expect further improvements in our signal-to-noise ratio and spectral results for this source with the future inclusion of data from the full detector area.

We thank G. Nystrom, V. Kuosmanen, J. Gomes, and other members of the SAO Engineering group for their support. We thank J. Braga for his important contributions to EXITE, E. Hegblom for assistance in analyzing these data, and J. McClintock for comments. We thank Robert Kubera and the NSBF field crew for their excellent balloon launch support. C. E. C. gratefully acknowledges the support of the NASA Graduate Student Researchers Program (CfA) and the Grainger Postdoctoral Fellowship (Chicago). This work was supported by NASA grant NAGW-624.

REFERENCES

- Braga, J., Covault, C. E., & Grindlay, J. E. 1989, *IEEE Trans. Nucl. Sci.*, A267, 212
- Covault, C. E. 1991, PhD thesis, Harvard University
- Covault, C. E., Grindlay, J. E., & Manandhar, R. P. 1990a, *BAAS*, 22 1320
- Covault, C. E., Grindlay, J. E., Manandhar, R. P., & Braga, J. 1990b, *Conference Record of the 1990 IEEE Nuclear Science Symposium*, 1, 515
- . 1991a, *IEEE Trans. Nucl. Sci.*, 38, 591
- Covault, C. E., Manandhar, R. P., & Grindlay, J. E. 1991b, *Proc. 22 Internat. Conf. on Cosmic Rays (Dublin)*, in press
- Dolan, J. F., Crannell, C. J., Dennis, B. R., & Orwig, L. E. 1987, *ApJ*, 322, 324
- Fenimore, E. E., & Canon, T. M. 1986, *Appl. Opt.*, 17, 337
- Finger, M. H. 1987, PhD thesis, California Institute of Technology
- Fishman, G. J., et al. 1991a, *IAU Circ.*, No. 5327
- Fishman, G. J., et al. 1991b, *IAU Circ.*, No. 5352
- Garcia, M. R., Grindlay, J. E., Burg, R., Murray, S. S., & Flanagan, J. 1986, *IEEE Trans. Nucl. Sci.*, 33, 750
- Grindlay, J. E., et al. 1978, *IAU Circ.*, No. 3238
- Grindlay, J. E., Covault, C. E., Kuosmanen, V., Gomes, J., Nystrom, G., & Manandhar, R. P. 1990, *Conference Record of the 1990 IEEE Nuclear Science Symposium*, 1, 493
- Grindlay, J. E., Garcia, M. R., Burg, R. I., & Murray, S. S. 1986, *IEEE Trans. Nucl. Sci.*, 33, 735
- Liang, E. P. T., & Nolan P. L. 1984, *Space Sci. Rev.*, 38, 353
- McClintock, J. E. 1991, in *Frontiers of X-ray Astronomy*, *Proc. 28th Yamada Conf. (Nagoya)*, ed. K. Koyama & Y. Tanaka, in press
- Miyamoto, S., et al. 1991, preprint
- Nolan, P. L., et al. 1982, *ApJ*, 262, 727
- Ricketts, M. J. 1982, *A&A*, 118, L3
- Skinner, G. K., et al. 1991, *A&A*, in press
- Sunyaev, R., et al. 1991a, *IAU Circ.*, No. 5204
- Sunyaev, R., et al. 1991b, *IAU Circ.*, No. 5342